# Combining Approximate Inverse and Joint Full Waveform Inversion for Velocity Model Building

Yubing Li, Romain Brossier, Ludovic Métivier

# Combining approximate inverse and joint full waveform inversion for velocity model building

Y. Li[1*], R. Brossier[1], L. Métivier[1,2]

[1] Univ. Grenoble Alpes, ISTerre, F-38058 Grenoble, France
[2] CNRS, Univ. Grenoble Alpes, LJK, F-38058 Grenoble, France

January 15, 2019

## Summary

Reflection waveform inversion (RWI) and its alternative - joint full waveform inversion (JFWI), are powerful tools for improving initial velocity model building beyond the diving-wave penetration depth. Such approaches rely on the scale separation between the smooth background model controlling the kinematics and the model perturbation characterizing the rapid local variations. The key difficulty in RWI and JFWI is the intensive computational cost introduced by alternating between the background velocity update and the model perturbation reconstruction. To update the background model at each step, a number of iterations are generally required to accurately reconstruct the model perturbation such that the alternating workflow becomes prohibitively expensive. To get rid of this computational intensity, we combine RWI or JFWI with efficient impedance waveform inversion which introduces the approximate inverse preconditioner. This approximate inverse approach contains only wave-equation-based operators and is formulated in the time domain.

## Introduction

Reflection waveform inversion (RWI) is a promising technique to build the velocity macromodel using reflection data (Xu et al., 2012; Brossier et al., 2015). It is inspired by the migration-based traveltime tomography (MBTT) approach (Chavent et al., 1994). RWI relies on the scale separation between the smooth background model controlling the kinematic and the perturbation model characterizing the rapid local variations. It either assumes an explicit split between low and high frequency content of the velocity model Xu et al. (2012) or introduces the velocity-impedance parameterization to naturally facilitate the separation Zhou et al. (2015). It leads to a workflow in which one repeatedly alternates two steps: the velocity macromodel is reconstructed assuming a known perturbation model and the perturbation model is updated using the previously retrieved velocity as the background model. Zhou et al. (2015) propose to extend RWI to joint full waveform inversion (JFWI) by considering both diving and reflected waves simultaneously. To retrieve the perturbation model, RWI and JFWI introduce the least-squares migration or similar techniques which generally require a number of iterations to converge such that the two-step workflow can become prohibitively expensive. It is one of the major bottlenecks preventing an efficient RWI or JFWI implementation, especially for the extension to 3D.

There are a few preconditioners designed to boost the convergence of least-squares data-fitting optimization problems. Among others, Métivier et al. (2015) combine the asymptotic operators proposed by Beylkin (1985) and full waveform inversion (FWI) for better conditioning the inverse problem. More recently, for more efficient FWI (Qin et al., 2015) or more robust velocity analysis (Li and Chauris, 2018), such operator is modified into a common-shot inverse formulation that contains only wave-equation-based operators in the frequency domain. This approximate inverse operator compensates for geometrical spreading and illumination in a pure wave-equation-based manner. In this paper, according to velocity-impedance parameterization, we first extend this operator to the time domain to allow calculating the model update on-the-fly, saying that no wavefield is required to be stored in the memory. Then, we couple the approach to impedance waveform inversion (IpWI) for preconditioning the perturbation model reconstruction in the two-step RWI or JFWI procedure. Finally, we apply the modified two-step strategy to Marmousi model and present the reconstructed velocity macromodel.

## Theory - preconditioner for IpWI

The acoustic wave equation controlling the seismic wave propagation in an isotropic medium reads

$$\Big(-\frac{\omega^2}{V_p I_p}-\nabla\cdot\frac{V_p}{I_p}\nabla\Big)u(s,x,\omega)=\Omega(\omega)\delta(x-s), \tag{1}$$

where $s$ is shot position, $\omega$ the angular frequency, $\Omega$ the source wavelet, and $u$ the wavefield. $V_p$ and $I_p$ denote the pressure velocity and impedance, respectively. Density $\rho$ is linked to $V_p$ and $I_p$ through $I_p = V_p\rho$. The perturbations can be expressed as $(\delta I, \delta V, \delta u) = (I_p - I_0, V_p - V_0, u - u_0)$. We consider the first-order Born approximation to linearize the wave equation:

$$\begin{aligned}\delta u(s,r,\omega)\approx\int \mathrm{d}x\,&\frac{V_0\delta v+I_0\delta I}{V_0 I_0}\omega^2\Omega(\omega)G_0(s,x,\omega)G_0(r,x,\omega)\\&+\frac{V_0\delta I-I_0\delta V}{V_0^2}\nabla G_0(r,x,\omega)\cdot\nabla G_0(s,x,\omega).\end{aligned} \tag{2}$$

Under the asymptotic assumption, the Green's function and its gradient read in the frequency domain:

$$G_0(s,x,\omega)=A_{sx}K(\omega)e^{i\omega\tau_{sx}};\ \nabla G_0(s,x,\omega)=i\omega G_0(s,x,\omega)\nabla\tau_{sx}, \tag{3}$$

where $A_{sx}$ denotes the amplitudes related, $K(\omega)$ equals to $1/\sqrt{i\omega}$ in 2D and to 1 in 3D, and $\tau_{sx}$ is the traveltime between $s$ and $x$. By substituting equation (3), we rearrange equation (2), reading

$$\delta u(s,r,\omega)=-\int \mathrm{d}x\,\omega^2\Omega(\omega)G_0(s,x,\omega)G_0(r,x,\omega)\frac{2}{V_0 I_0}\Big(\frac{\delta V}{V_0}\sin^2\theta+\frac{\delta I}{I_0}\cos^2\theta\Big), \tag{4}$$

where $\theta$ denotes the half scattering angle at imaging point $x$. Note that this formulation is another illustration of the idea of Zhou et al. (2015) that velocity and impedance are naturally separated parameters in terms of diffraction patterns. For short offsets where $\theta$ is small, saying $\cos\theta\approx 1$ and $\sin\theta\approx 0$, we define a shot-dependent parameter $\xi(x,s)=2\delta I/(V_0 I_0^2)$ and introduce the asymptotic expression of

Green's function to rewrite equation (4), resulting in

$$\delta u(s,r,\omega) \approx -\int \mathrm{d}x\, \omega^2 \Omega(\omega) \xi(x,s) A_{sx} A_{rx} K(\omega) K(\omega) e^{i\omega(\tau_{sx}+\tau_{rx})}, \tag{5}$$

such that the asymptotic inverse proposed by Beylkin (1985) can be applied, yielding

$$\xi(x,s) \approx -\iint \mathrm{d}r\mathrm{d}\omega\, \frac{4}{V_0^2} \frac{\cos\beta_r}{V_r} \cos^2\theta \frac{1}{\Omega(\omega)} \frac{K^*(\omega) A_{rx}}{K(\omega) A_{sx}} \delta u(s,r,\omega) e^{-i\omega(\tau_{sx}+\tau_{rx})}, \tag{6}$$

where $\beta_r$ and $V_r$ are the oriented angle and velocity at the receiver position, respectively. Li and Chauris (2018) rewrite this formulation with only wave-equation-based operators in the frequency domain and we extend it to the time domain, reading,

$$\xi(x,s) = -\int \mathrm{d}\omega\, \frac{4}{(i\omega)^3} \frac{\Omega^*(\omega) \nabla G_0^*(s,x,\omega) \cdot \nabla R(s,x,\omega) + (\frac{i\omega}{V_0})^2 \Omega^*(\omega) G_0^*(s,x,\omega) R(s,x,\omega)}{\Omega(\omega) G_0(s,x,\omega) \Omega^*(\omega) G_0^*(s,x,\omega)} \tag{7}$$

$$= -\frac{1}{A_{sx}^2} \int \mathrm{d}\omega\, \frac{4}{(i\omega)^3} \frac{1}{\Omega(\omega)} \left( \nabla G_0^*(s,x,\omega) \cdot \nabla R(s,x,\omega) + (\frac{i\omega}{V_0})^2 G_0^*(s,x,\omega) R(s,x,\omega) \right) \tag{8}$$

$$\approx \frac{\nabla S(s,x,t) \star \nabla R(s,x,t) + \frac{1}{V_0^2} \frac{\partial^2}{\partial t^2} S(s,x,t) \star R(s,x,t)}{G_0(s,x,t) \star G_0(s,x,t)}, \tag{9}$$

where $*$ denotes the adjoint operator and $\star$ the zero lag cross correlation. Incident and adjoint wavefields are defined as

$$S(s,x,\omega) = \frac{4}{(i\omega)^3} \frac{1}{\Omega^*(\omega)} G_0(s,x,\omega); R(s,x,\omega) = \int \mathrm{d}r\, \frac{\partial G_0^*(r,x,\omega)}{\partial r_z} \delta u(s,r,\omega). \tag{10}$$

It is important to notice that the amplitude term in the asymptotic expression of Green's function is frequency-independent which allows us to transfer the frequency-domain formulation (7) to the time-domain expression (9). Equations (7) to (10) are presented only in 3D case for simplicity. To apply the above theory to IpWI, two points are essential: (1) the velocity model is fixed such that the perturbation of velocity model $\delta V = 0$; (2) the IpWI approach only uses reflection data at short-offsets where $\theta$ is considered to be small.

**Theory - macro velocity update**

With the impedance reconstructed by preconditioned IpWI, we minimize the following objective function to update the velocity macromodel

$$J_{JFWI}(V_p) = \frac{1}{2} \left\| W^r \left( d_{obs} - d_{cal}(V_p, I_p) \right) \right\|_2^2 + \frac{1}{2} \left\| W^d \left( d_{obs} - d_{cal}(V_p, I_p) \right) \right\|_2^2, \tag{11}$$

where $d_{obs}$, $d_{cal}$ denote the observed and calculated data, respectively. $W^r$ and $W^d$ are weighting functions to roughly select reflected and diving waves, respectively. The gradient of the objective function with respect to the macro velocity $V_p$ reads

$$\nabla J_{JFWI} = \sum_{s,r} (u_0 \star \delta\lambda^r + \delta u \star \lambda_0^r + \delta u \star \delta\lambda^r + u_0 \star \lambda_0^d), \tag{12}$$

where $\lambda_0^d$ and $\lambda_0^r$ denote the background adjoint wavefield generated by the diving and reflected wave residuals, respectively. $\delta\lambda^d$ and $\delta\lambda^r$ are the scattered adjoint wavefields associated with the diving and reflected wave residuals, respectively. Note that one can simply remove the terms $\frac{1}{2}\|W^d(d_{obs} - d_{cal})\|_2^2$ and $u_0 \star \lambda_0^d$ in equations (11) and (12) to derive the RWI theory. See Zhou et al. (2015) for more details about the RWI and JFWI theories.

**Results - IpWI**

We first compare the conventional depth preconditioner with the approximate inverse preconditioner proposed here for the Marmousi model. By depth preconditioner, we mean multiplying the IpWI gradient by the depth value. On the other hand, we use equation (9) to calculate the preconditioned gradient in the approximate inverse preconditioner case. We trigger 64 shots located at the surface from 0.1 to 10.18 km. The shot interval is 0.16 km. For each shot, receivers are deployed on the right side of the shot with offsets ranging from 0 to 3.0 km. The source function is a Ricker wavelet of which the maximal

frequency is 10 Hz. We also filtered out the contents below 2 Hz in the source wavelet. We apply a Gaussian smoothing filter to the true $V_p$ and $I_p$ models to generate the initial models (Figures 1a and 1b). The characteristic length of Gaussian filter equals to twice the minimal wavelength of the observed data. We apply a time-dependent filter to the data-fitting objective function to remove direct arrivals and to select reflected waves of which the offsets are less than 1.0 km. We apply the non-linear conjugate gradient method for inversion. The approximate inverse preconditioner helps IpWI converge much faster than in the depth preconditioner case (Figure 1c). Compared to the exact $I_p$ model (Figure 1d), the retrieved $I_p$ model after 10 depth preconditioned iterations (Figure 1e) are poorly reconstructed in the deep part. On the other hand, it is remarkable that the approach proposed here can provide more details about reflectors below 2.5 km after only one single iteration.

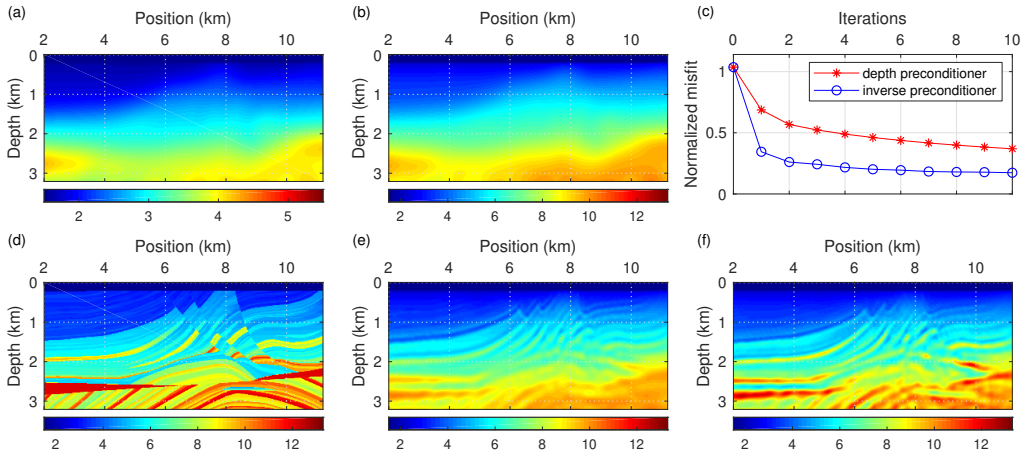


***Figure 1*** *Comparison between conventional method and the proposed approach: initial $V_p$ (a); initial $I_p$ (b); true $I_p$ (d); reconstructed $I_p$ after 10 iterations of depth preconditioned IpWI (e); reconstructed $I_p$ after 1 iteration of approximate inverse preconditioned IpWI (f). The misfit value decreases along iterations (c) in both cases.*

## Results - RWI and JFWI

We use the same source wavelet, initial models and streamer acquisition system as in the previous section. We select reflected data at offsets less than 1.0 km for IpWI and full-offset data for subsequent macro velocity updates. Compared to the exact $V_p$ model (Figure 2), RWI and JFWI both retrieves the background components of the $V_p$ model (Figures 2b and 2c) after a few cycles, starting from the initial model generated by applying a strong smoothing filter to the true model. By cycle, we mean a combination of 3 iterations of IpWI and 20 iterations of RWI or JFWI. The JFWI result better constrains the shallower part than in the RWI case because the diving waves are considered. Starting from the $V_p$ model in Figure 1a, standard FWI recovers a $V_p$ model in which the deep layers are not located at correct depths (Figure 2d). On the other hand, considering the RWI or JFWI results as the initial model, the $V_p$ models reconstructed by FWI (Figure 2e and 2f) do not suffer from the same problem. The model profile (Figure 2g) illustrates that the layers between 2.5 and 2.8 km are not properly positioned in the FWI case. The RWI followed by FWI strategy positions the layers at correct depths but the values of velocity require more iterations to recover. Nevertheless, the JFWI followed by FWI strategy has better-reconstructed both the values and positions of these layers than in the previous cases.

## Conclusions and Perspectives

We have proposed to couple the approximate inverse preconditioner to impedance waveform inversion for an efficient RWI or JFWI workflow. The time-domain approximate inverse preconditioner boosts the convergence speed of the IpWI procedure. The preconditioner is implemented in a pure wave-equation-based manner and introduces no additional memory requirements. In addition, the reconstructed impedance using the approximate inverse preconditioner consists of sharper layer contrasts than in the conventional case. Consequently, the efficiency of RWI and JFWI has been significantly improved. In the Marmousi model case, under the streamer acquisition with a limited offset range, RWI

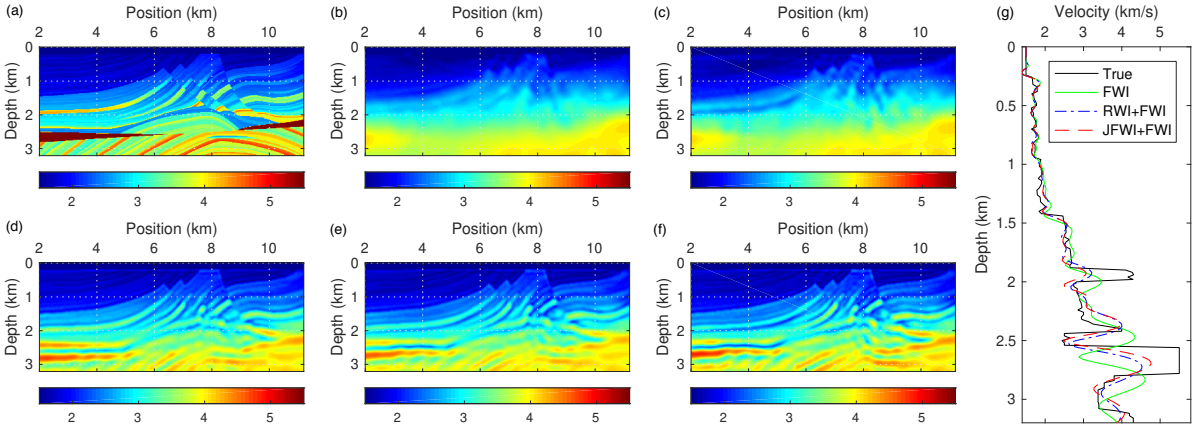


***Figure 2*** *Comparison between true model and inversion results: true $V_p$ (a); reconstructed $V_p$ after 20 RWI cycles (b); reconstructed $V_p$ after 15 JFWI cycles (c); reconstructed $V_p$ after 50 FWI iterations (d); reconstructed $V_p$ after 50 FWI iterations using RWI result (e) or JFWI result (f) as the initial model. $V_p$ in Figure 1a is used as initial model for (b-d). Depth preconditioner is applied in (d-f). The comparison of profiles at $x = 3$ km is shown in (g).*

or JFWI has built a good starting model for subsequent FWI, in the sense that the final velocity model recovered by FWI is closer to the true model than in the conventional case. We have observed that the macro velocity update step requires 20 iterations to converge at the beginning, but the required number of iterations decreases cycle by cycle and only 3 iterations are sufficient in the final stage. It means that a stopping criteria can be introduced to further reduce the computational cost in the future. The subsequent work consists of the extension to 3D and of the application to real streamer data.

## Acknowledgments

This study was partially funded by the SEISCOPE consortium (http://seiscope2.osug.fr), sponsored by AKERBP, CGG, CHEVRON, EQUINOR, EXXON-MOBIL, JGI, PETROBRAS, SCHLUMBERGER, SHELL, SINOPEC and TOTAL. This study was granted access to the HPC resources of CIMENT infrastructure (https://ciment.ujf-grenoble.fr) and CINES/IDRIS/TGCC under the allocation 046091 made by GENCI.

## References

Beylkin, G. [1985] Imaging of discontinuities in the inverse scaterring problem by inversion of a causal generalized Radon transform. *Journal of Mathematical Physics*, **26**, 99–108.

Brossier, R., Operto, S. and Virieux, J. [2015] Velocity model building from seismic reflection data by full waveform inversion. *Geophysical Prospecting*, **63**, 354–367.

Chavent, G., Clément, F. and Gòmez, S. [1994] Automatic determination of velocities via migration-based traveltime waveform inversion: A synthetic data example. *SEG Technical Program Expanded Abstracts 1994*, 1179–1182.

Li, Y. and Chauris, H. [2018] Coupling direct inversion to common-shot image-domain velocity analysis. *Geophysics*, **83**(5), R497–R514.

Métivier, L., Brossier, R. and Virieux, J. [2015] Combining asymptotic linearized inversion and full waveform inversion. *Geophysical Journal International*, **201**(3), 1682–1703.

Qin, B., Allemand, T. and Lambaré, G. [2015] Full waveform inversion using preserved amplitude reverse time migration. In: *SEG Technical Program Expanded Abstracts 2015*. 1252–1257.

Xu, S., Wang, D., Chen, F., Lambaré, G. and Zhang, Y. [2012] Inversion on Reflected Seismic Wave. *SEG Technical Program Expanded Abstracts 2012*, 1–7.

Zhou, W., Brossier, R., Operto, S. and Virieux, J. [2015] Full Waveform Inversion of Diving & Reflected Waves for Velocity Model Building with Impedance Inversion Based on Scale Separation. *Geophysical Journal International*, **202**(3), 1535–1554.